Quantitative Analysis and High-Resolution X-ray Mapping with a Field Emission Electron Microprobe

C. Hombourger* **and M. Outrequin**
Cameca SA, 29 Quai des Grésillons, 92622 Gennevilliers Cedex, France
*chrystel.hombourger@ametek.com

Introduction

The electron probe microanalyzer (EPMA) provides quantitative analysis for nearly all chemical elements with a spatial resolution of analysis about ~1 µm, which is relevant to microstructures in a wide variety of materials and mineral specimens. Recent implementation of the Schottky emitter field-emission gun (FEG) electron source in the EPMA has significantly improved the spatial resolution and detectability of the EPMA technique.

A major benefit of the Schottky emitter is that it can provide a highly focused electron beam containing large beam currents even at low beam energy. At low beam energy (<10 keV), the interaction volume—within which scattered electrons generate X rays—decreases to the sub-µm scale compared to the conventional micrometer-level EPMA analysis at 15 or 20 keV. The spatial resolution for X-ray analysis also depends on the density of the specimen material. It is thus recommended to use a Monte Carlo simulation program to model the interaction volume and estimate the spatial resolution [1, 2].

Because X rays are generated from a much larger diameter than the diameter of the incident electron beam, it is advisable to optimize the two interdependent parameters, accelerating voltage and beam diameter, to take full advantage of the FEG electron source for X-ray analysis. Optimized conditions are obtained when the analytical spatial resolution is primarily limited to the diameter of the X-ray emission volume in a specific material.

At low beam energy, only X-ray lines of low energy are excited, such as K lines for atomic numbers lower than 22 and L and M lines for atomic numbers greater than 22. Low beam energy operation (that is, <5 keV) offers several advantages: it improves the analytical spatial resolution, reduces the contribution of secondary fluorescence, and decreases charging effects. However, it can become a challenge because X-ray lines of low energy are subject to peak shift, the lines excited in this energy region often overlap, absorption of soft X ray in high-Z elements makes calculation of composition difficult, and the fluorescence yields of L and M lines are lower than for the K lines. The latter problem is often responsible for low intensities of certain lines, as is the likely low overvoltage U, defined as the ratio of beam energy to ionization energy for a line, which may reduce the ionization probability for a particular X-ray line [1].

A major strength of the EPMA is its ability to accurately quantify elements down to trace concentrations of a few ppm. The Schottky FEG allows trace element analysis because of the high beam currents available and the excellent stability of the beam current. The quality of a quantification depends critically on the stability of the beam current and on the reproducibility, sensitivity, and spectral resolution of the wavelength dispersive spectrometers (WDSs) employed to measure X rays in the EPMA.

In this article we present several examples of FE-EPMA analyses acquired on the CAMECA SX Five FE. This EPMA, equipped with a Schottky FEG source, provides quantitative and repeatable analyses at high analytical spatial resolution.

Factors Affecting Analytical Spatial Resolution

Analytical spatial resolution is defined as the quadratic sum of the diameter of the beam and the diameter of the X-ray emission volume [3]. It is thus related to the beam energy, the beam current selected, and the density of the specimen material.

The electron beam density achieved with a field-emission source is much greater compared to that obtained with conventional W/LaB_6 sources; thus, small beam diameters can be obtained with high beam currents. The electron beam diameter may be measured (Figure 1) from a line scan traversing a sharp phase boundary, as the width of a step in electron signal intensity at 16%–84% of the total signal amplitude [4]. This method has been applied to perform beam diameter measurements at different beam voltages and beam currents as shown, for example in Figure 2. This figure shows that at a given electron beam energy, the lower the beam current, the smaller the electron beam diameter [5]. The overall shape of the curves in Figure 2 is a consequence of increasing chromatic aberration effects at lower electron beam energies [1].

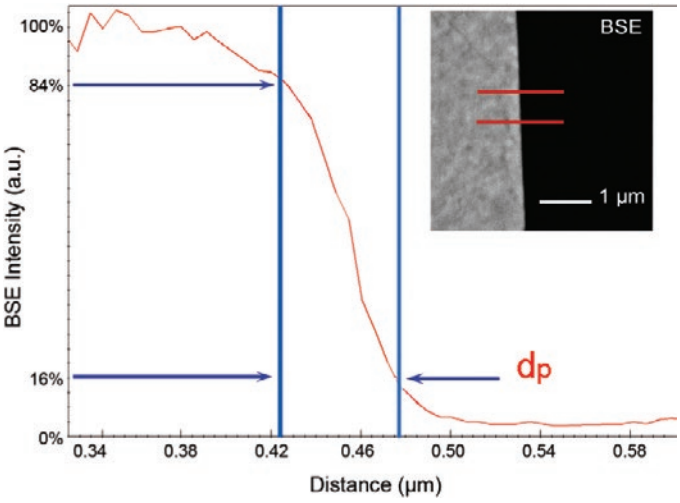

Figure 1: Intensity change in a BSE line scan across an Fe/VC phase boundary in a superalloy (inset). The BSE signal was taken from within the red lines overlaid on the BSE picture. The estimated beam width was taken as the width d_p of the signal step between 84% and 16% of full intensity.

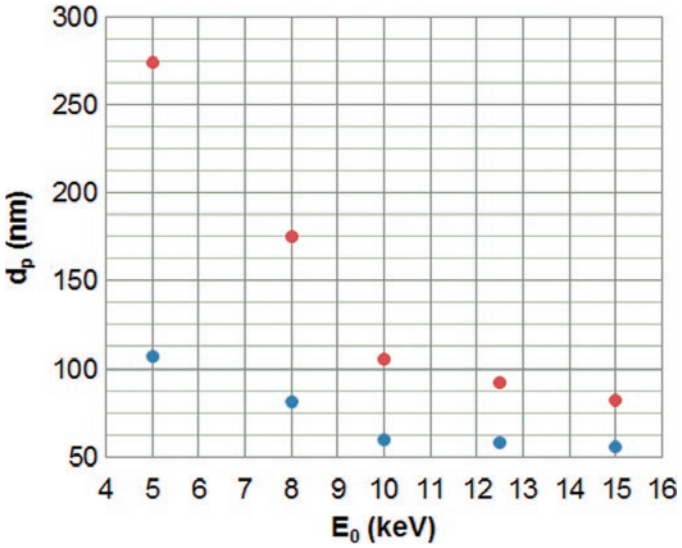

Figure 2: Beam diameter versus beam accelerating voltage at 2 beam currents (blue = 10 nA, red = 100 nA). As a comparison, with a W filament the beam diameter would be d_p = 600 nm at 15 keV and 100 nA.

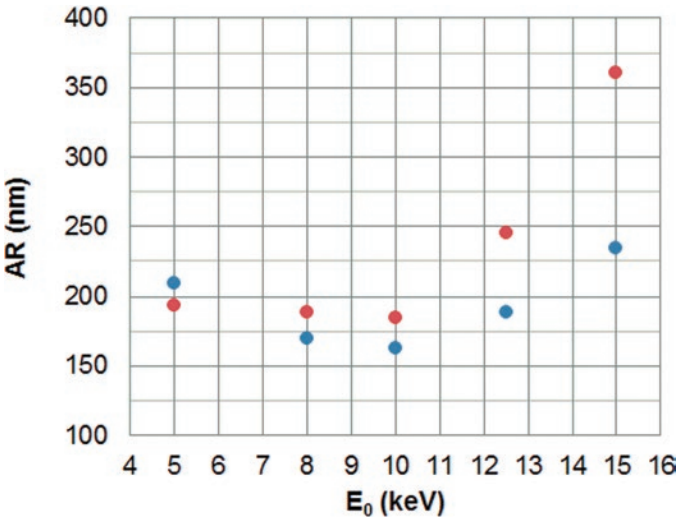

Figure 4: Analytical resolution (AR) for the Fe La (blue) and V La (red) lines measured at 10 nA for 5 impact energies at a sharp interface. The analytical resolution was measured as shown in Figure 1. As a comparison, for the Fe Kα line excited with a 15 keV beam, the analytical resolution would be about 1 µm.

For a beam of constant diameter entering the specimen, the lower the beam impact energy, the smaller the interaction volume, and the better the analytical spatial resolution. This effect can be visualized by running a Monte Carlo simulation of the process (Figure 3, for example with the free program CASINO [2]). The yellow portions of the trajectories show where incident electrons still have enough energy to excite Al K-series X rays. The analytical spatial resolution decreases (improves) by about 60% from 10 keV to 5 keV.

For a given material, improvement of analytical resolution requires a balance between beam energy and the diameter of the incident electron beam as shown on Figure 4 for a V-Cr-Fe superalloy. The analytical resolutions for the Lα lines of Fe and V were measured at 16% and 84% of the total X-ray signal from the line scan across the sharp interface shown on Figure 1 at a beam current of 10 nA for 5 impact energies (5, 8, 10, 12.5, and 15 keV). In this superalloy, the best spatial resolution was achieved at 10 keV primary electron energy.

Figure 5 presents X-ray maps that show the influence of electron beam energy on the analytical spatial resolution at constant beam diameter. As expected from the Monte Carlo simulations, these Al Kα maps acquired at progressively lower electron beam energies show that the best image resolution is obtained at the lowest beam energy. At 5 keV the Si-rich phases (black regions) are well resolved, whereas they are difficult to distinguish under conventional microanalysis conditions of 10–15 keV. In this experiment, the beam diameter was kept constant at 80 nm by readjusting the beam current for each beam energy; thus the differences in the maps are entirely attributable to the variations in the interaction volume at each beam energy.

Beam current and beam energy also affect quantitative analysis precision. In case of trace element analysis, the optimum analytical conditions for achieving the greatest precision are not compatible with the highest lateral spatial resolution. Trace element analysis requires high beam currents in the range of 100 to 200 nA and often higher beam energies to produce as many X-ray counts as possible for the element of interest. Thus, to optimize measurement precision and detection limits, a poorer spatial resolution must be accepted [3].

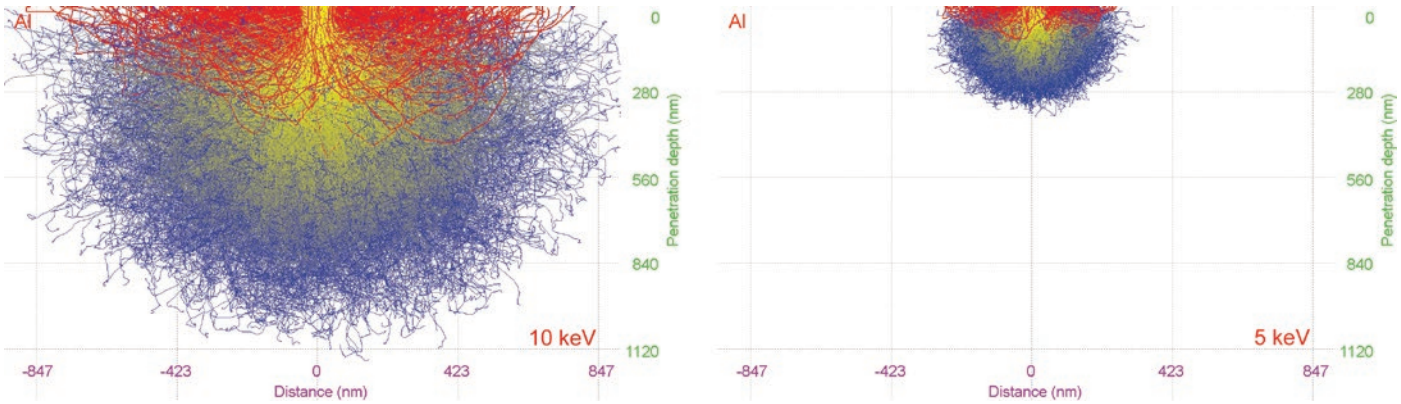

Figure 3: Monte Carlo simulations of electron trajectories beneath the aluminum specimen surface as calculated by CASINO [2]. Note the decrease in the interaction volume for Al as the beam energy decreases from 10 keV to 5 keV (red = backscattered electrons, yellow = other electrons of high energy, blue = electrons of low energy).

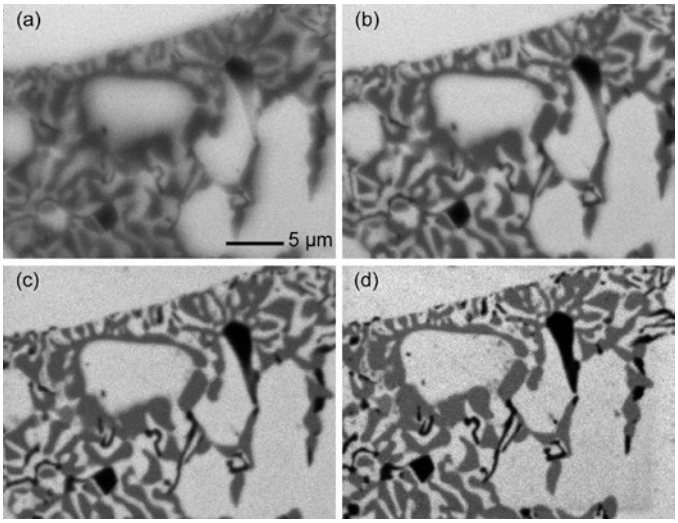

Figure 5: X-ray maps of Al Kα line acquired with FE-EPMA at (a) 15 keV, (b) 10 keV, (c) 7 keV, and (d) 5 keV for a beam diameter of 80 nm. Specimen is an aluminum bronze, and each map was acquired over 33 minutes.

Quantitative Analysis: Long-term Stability and Repeatability

A key figure of merit for any analytical tool like the EPMA is to provide reliable quantitative data. Figure 6 shows results from a long-term stability experiment on a 316L stainless steel specimen conducted over 11 weeks. Each point in these figures is the average of 6 measurements performed on the same day. During the period of the test, the WDSs were not recalibrated, and the specimen was removed from the FE-EPMA between successive measurements. The experiment was conducted at 15 keV and 20 nA with a counting time of 20 s at peak and background spectral positions.

Table 1 shows the quantitative analysis of major (Fe, Cr, and Ni) and minor (Mn, Mo, and Si) elements along with ±1 σ standard deviations. Measurement stabilities of 0.2 wt% for iron ([Fe] = 67.08 wt%) and 0.01 wt% for silicon ([Si] = 0.59 wt%) were achieved. The quality of these data was achieved thanks to closed-loop beam current control and a WDS design providing high reproducibility, high sensitivity, and high spectral resolution.

Table 1: Measurement stability shown by quantification of elements in a 316L stainless steel specimen over 11 weeks (see Figure 6).

Element	Measured Conc. wt%	Precision ±1σ wt%
Fe	67.08	0.21
Cr	17.81	0.06
Ni	11.25	0.10
Mo	2.07	0.04
Mn	1.46	0.03
Si	0.59	0.01
Total	100.26	

Quantitative Analysis of Precipitates at Low Beam Energy

The ability to accurately quantify ever-smaller precipitate phases when working at low beam energy (6 keV) and low beam current (20 nA) is illustrated in Figure 7. These results show quantitative analyses for precipitates ranging from 0.3 µm to 2.5 µm in diameter in a matrix of Mg-Pd. For sizes above 0.6 µm in diameter, concentrations of Mg, Cu, and Pd are flat and stable indicating that the X rays are coming only from the precipitate phase. Below 0.6 µm in diameter, signals from Pd and Mg increase and the Cu signal decreases, indicating that those precipitates were smaller than the analyzed volume.

Figure 8 shows an X-ray map of the Cu Lα line acquired from this specimen under the same excitation conditions as the quantitative analysis. This map shows particles typical of the analysis and a 0.6 µm particle (Figure 8b) within the size range for the expected composition.

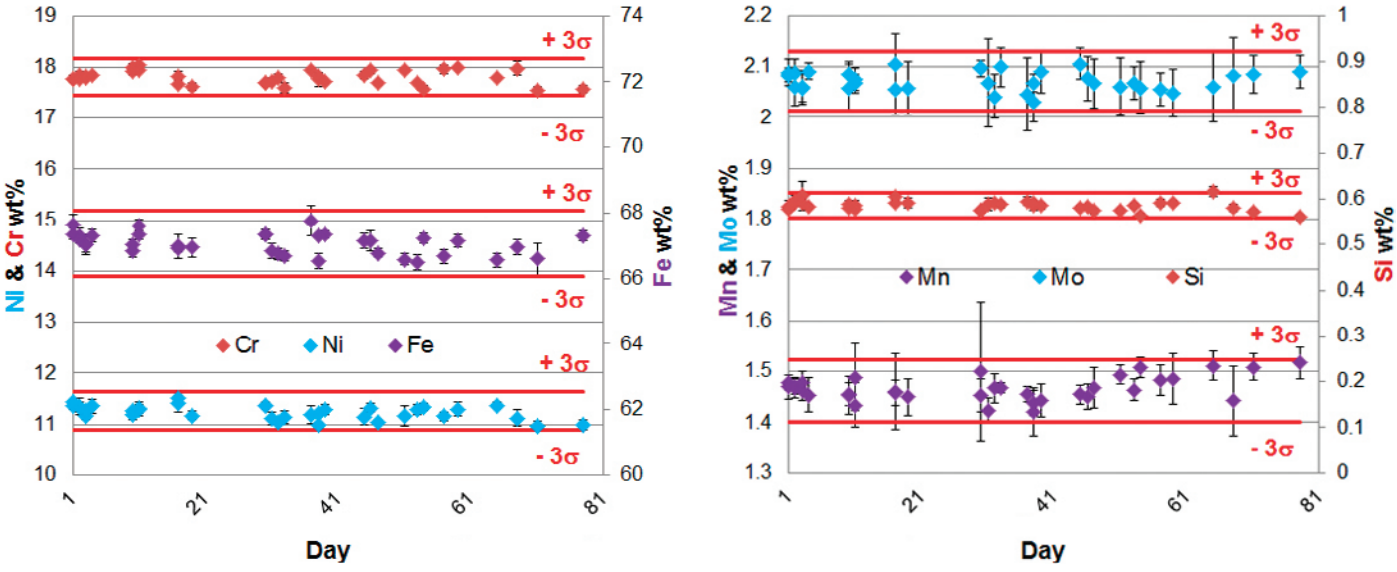

Figure 6: Long-term stability of repeated measurements over 11 weeks on the same specimen of 316L stainless steel.

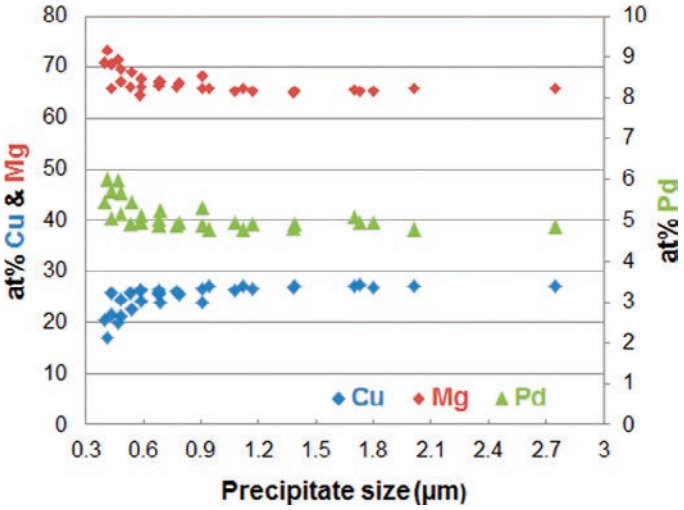

Figure 7: Quantitative analyses of small Cu-Mg-Pd precipitates in a Mg-Pd matrix at a beam energy of 6 keV and beam current of 20 nA. Sample courtesy of Dr. Eric Leroy, CNRS ICMPE, Thiais, France.

High-Resolution X-ray Mapping

Small intermediate phases in geological specimens, typically a few hundreds of nanometers in extent, can be identified on an elemental X-ray map. For a clear and unambiguous identification of individual phases, it is necessary to optimize the analytical resolution by lowering beam energy and reducing the diameter of the electron beam.

Figure 9 shows X-ray elemental maps for Fe, Mg, Ti, and Nb acquired with 6 keV beam energy from a composite Fe-Ti oxide phase from a metasomatized peridotite xenolith in basalts from South East Siberia. The maps show evidence of exsolution lamellae of Nb-bearing rutile (TiO_2 with low Fe_2O_3 content) rimmed with ilmenite ($FeTiO_3$) enclosed by hematite (Fe_2O_3).

To quantify the analytical resolution achieved at 6 keV on this specimen, an X-ray line scan was acquired across the specimen (see the white line on the Fe map). At 6 keV, the Fe L-series, Mg K-series, and Nb L-series are excited with an overvoltage greater than 2, while the Ti K-series is excited at a lower overvoltage of 1.2. Figure 10 shows line scans for Ti Kα and Fe Lα taken across the hematite-ilmenite-rutile interface. Measuring the width between the 16% and 84% signal levels along this Ti Kα line scan yields a 310 nm analytical spatial resolution.

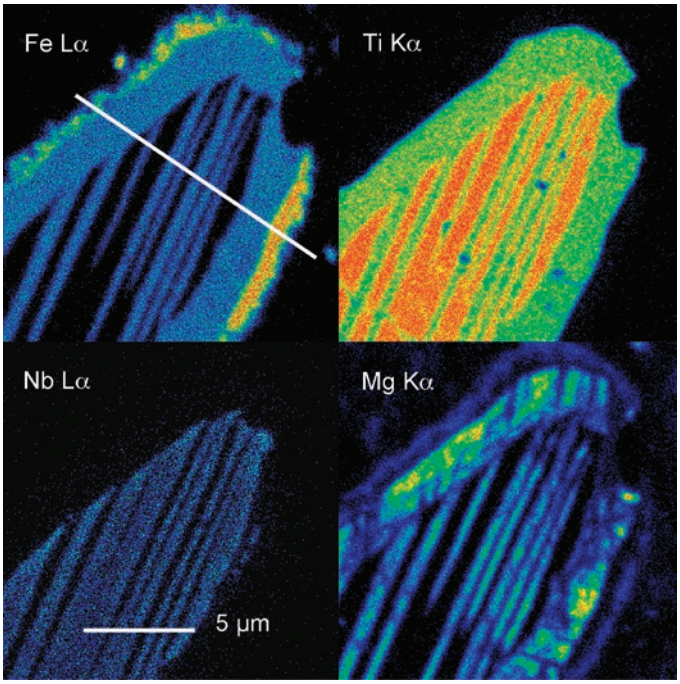

Figure 9: X-ray maps of Ti Kα, Nb Lα, Mg Kα, and Fe Lα lines of hematite-ilmenite-rutile sample obtained at 6 keV and 50 nA. Sample courtesy of F. Kalfoun, D. Ionov, and C. Merlet [8].

Trace Analysis and Detectability Limits

Because of its accuracy, precision, and non-destructive characteristics, the EPMA is one of the instruments of choice for quantifying trace elements in the geochemistry of monazite, a phosphate mineral typically containing rare earth elements (REE) including La, Ce, Pr, and Nd. In certain varieties of this mineral, thorium is present at relatively significant concentrations, whereas uranium and lead are present at variable and low concentrations. The measurement of U, Th, and Pb concentrations allows monazite dating [6]. When dealing with trace element analysis, the analyst must optimize various interdependent analytical parameters such as beam conditions, analytical spatial resolution, spectral analysis (energy resolution, background positions, interferences, etc.), and analysis time. To achieve the sensitivity and the precision required for the desired analysis, it is necessary to pay attention to all of these parameters.

Experimental conditions. For monazite the best compromise for optimizing the lateral spatial resolution, while detecting all the elements (majors and minors), is a beam energy of 10 keV and a high beam current in the range of 100 to 200 nA [3].

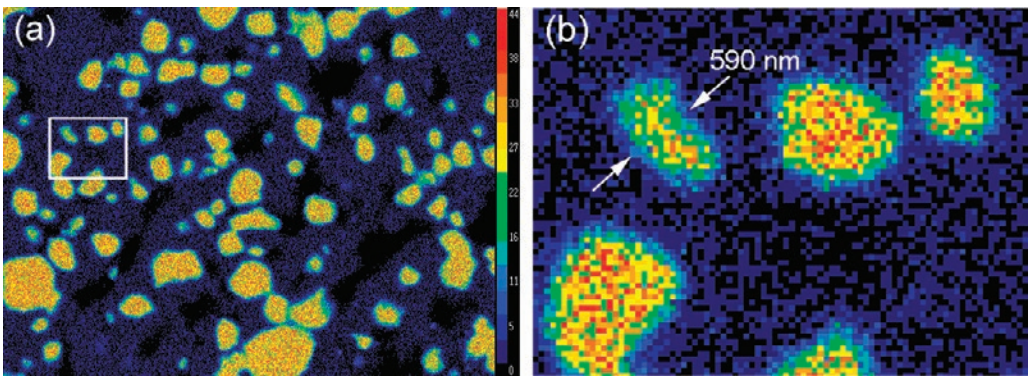

Figure 8: X-ray map of the Cu Lα line from the small Cu-Pd-Mg precipitates with electron energy of 6 keV and electron beam current of 20 nA. Image collected by scanning the beam. (a) Full mapped area. Total image width = 30 μm. (b) White rectangle area magnified. Image width = 5 μm. Sample courtesy of Dr. Eric Leroy, CNRS ICMPE, Thiais, France.

Spectral line selection. With a beam accelerating voltage of 10 keV, the L-line series will be excited for each REE. Because these elements may exhibit more than 10 lines in each L spectrum, great care is required in evaluating the peak interferences and in finding peak-free regions for background measurements. Figure 11 shows a typical monazite X-ray spectrum collected at 10 keV and 200 nA with a WDS equipped with a LPET (large pentaerythritol) crystal. The REEs like Ce, La, Nd, and Pr identified in this spectrum have X-ray lines very close to each other, presenting serious peak interferences. Elements like thorium and uranium are also shown in this spectrum. Because of the low concentrations, the most intense lines are generally chosen. In the case of serious peak interferences like U Mα and Th Mβ, however, X-ray lines of lower intensity like the Mβ line for uranium must be selected in order to achieve accuracy and precision. When selection of an interference-free peak is not possible, an overlap correction program may be used to eliminate the interfering line.

Spectral resolution. As a comparison, Figure 11 also shows a spectrum acquired on the same grain with an energy-dispersive X-ray spectrometer (EDS). Spectral resolution, the ability to resolve two X-ray lines, is at least an order of magnitude better with WDS than with EDS, which allows the separation of U Mβ and Th Mγ. Thanks to its superior energy resolution and peak-to-background ratio, shown in Table 2, WDS is definitely the technique of choice to perform accurate trace element analysis in monazite.

Peak-to-background ratio. When dealing with trace element analysis, peak-to-background ratio is an important factor because the detection limit [7] is also dependent on this P/B ratio expressed as

$$C_{min} = \left(\frac{C_{Std}}{(P_{Std}/B_{Std} - 1)}\right) * \frac{1}{B_{Std}} ZAF * \left(\frac{\lambda(\alpha,\beta)}{2t_S}\sqrt{1 + \frac{4B_S t_S (1 + 1/\gamma_S)}{\lambda(\alpha, \beta)}}\right)$$

where C_{Std} is the concentration in the standard, P_{Std} is the intensity at spectral peak position of the standard, ZAF is the matrix correction factor, B_{Std} is the intensity of the background at spectral peak position of the standard, t_S is the counting time at spectral peak position on the sample, B_S is the intensity of the background at spectral peak position of the sample, γ_S is the ratio of the counting times of background to peak spectral positions on the sample, and $\lambda(\alpha,\beta)$ is the statistical confidence level [9] to consider with a probability α that a concentration is >0 when $C = 0$ and with the probability β that the concentration equals 0 when in fact $C > 0$.

For a given concentration, the higher the P/B ratio, the better the detection limit at 95% confidence level (e.g. $\lambda(\alpha,\beta) = 13.0$), as shown in Table 2, which compares the P/B ratio for some X-ray lines

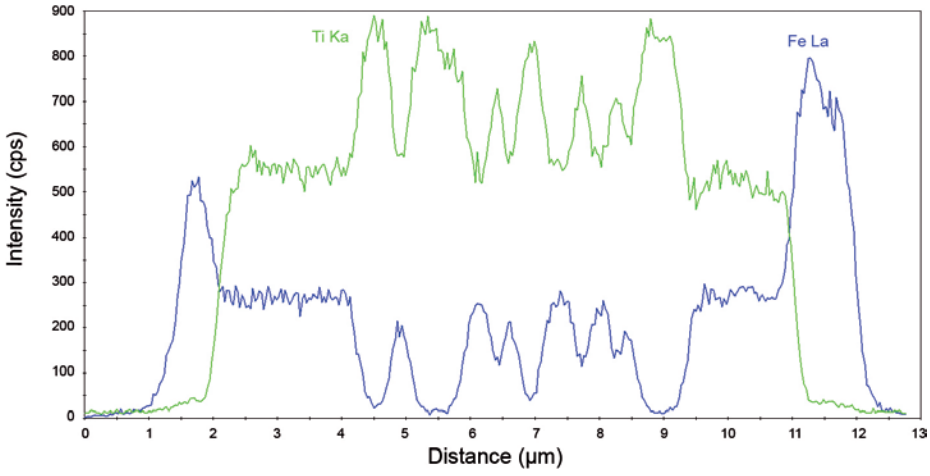

Figure 10: X-ray line scans across the hematite-ilmenite-rutile interface obtained at 6 keV. The spatial resolution extracted from the Ti Kα line scan was 310 nm when measured in the manner of Figure 1. Sample courtesy of F. Kalfoun, D. Ionov, and C. Merlet [8].

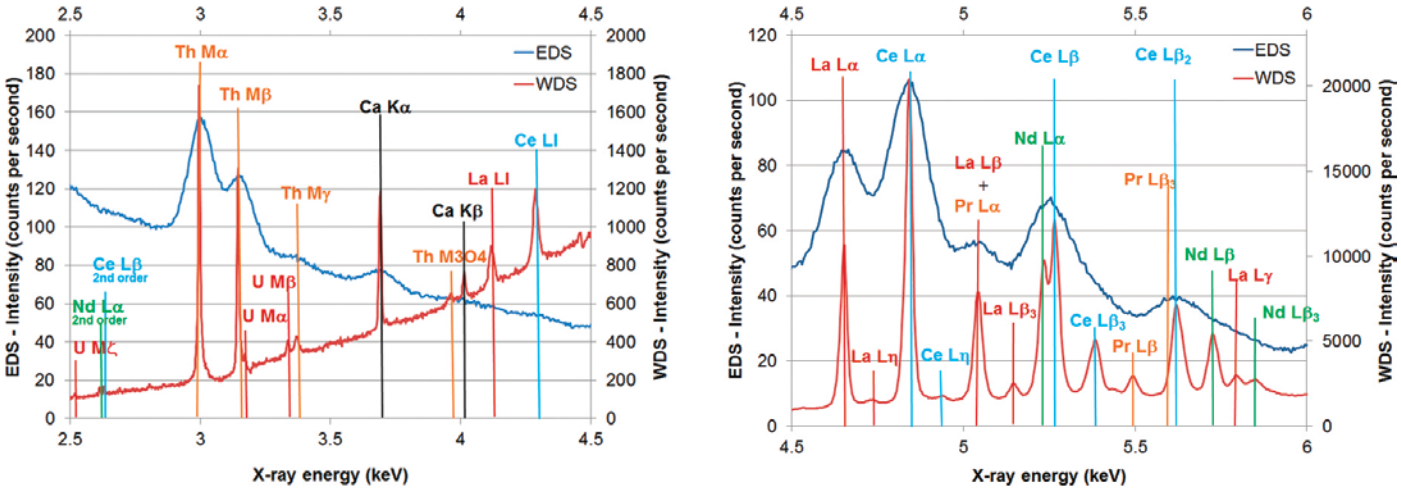

Figure 11: WDS (red line) and EDS (blue line) spectra obtained from a monazite grain at 10 keV and 200 nA. Sample courtesy of Dr. Grzegorz Zielinski, PIG, Poland.

Table 2: Comparison of energy resolution ΔE (eV), peak-to-background ratio and minimum detectability limit (DL) for selected elements present in a Monazite-Ce grain using detection by WDS and EDS. Experimental conditions: 10 keV, 100 nA, beam diameter of 105 nm; EDS data collected at 138 kcps for 60 s with a 19% dead time; WDS data collected for 30 s at peak and background positions for each element.

Analysis	X-ray line	ΔE (eV)	P (cps)	B (cps)	P/B	Conc. (wt%)	DL (wt%) [7]
WDS	Ca Kα	11.2	565	198	2.84	0.38	0.0137
	La Lα	21.9	4948	560	8.83	12.47	0.0626
	Th Mα	8.6	1123	89	12.59	7.24	0.0616
	Ce Lα	23.9	9932	721	13.77	24.51	0.0666
	U Mβ	12.3	203	169	1.2	0.38	0.0360
EDS	Ca Kα	114.0	78	69	1.13	—	0.0583
	La Lα	123.0	84	63	1.33	—	0.7605
	Th Mα	111.0	158	106	1.49	—	0.6523
	Ce Lα	135.0	105	63	1.67	—	1.5722

detected with WDS and EDS on a monazite-Ce grain. This table shows that the best detection limit is achieved with WDS for this material.

Conclusions

The data presented in this article show the advantages of employing a Schottky field-emission source in an EPMA. Specifically, data acquired with the Schottky field-emission-gun EPMA demonstrate sub-micrometer analytical spatial resolution at low beam energies. In combination with stable WDSs, this system provides element detectability at 10 keV in the 100 ppm range for certain elements in monazite, a difficult specimen with severe peak overlaps.

Acknowledgments

The authors would like to thank Dr. Ian Holton of Acutance Scientific Ltd and Dr. Charles. E. Lyman for reviewing the article and for fruitful discussions.

References

[1] JI Goldstein, DE Newbury, DC Joy, CE Lyman, P Echlin, E Lifshin, L Sawyer, and JR Michael. *Scanning Electron Microscopy and X-ray Microanalysis* (3rd ed.), Springer, New York, 2003.

[2] D Drouin, A Réal Couture, D Joly, X Tastet, V Aimez, and R Gauvin, *Scanning* 29 (2007) 92–101.

[3] MJ Jercinovic et al., *Chemical Geology* 254 (2008) 197–215.

[4] KD Cummings, LR Harriott, GC Chi, and FW Ostermayer, Jr., *SPIE* 632 (1986) 93–96.

[5] RFW Pease and WC Nixon, *J Sci Inst* 42 (1965) 81–85.

[6] ML Williams, MJ Jercinovic, and MP Terry, *Geology* 27 (1999) 1023–26.

[7] M Ancey, F Bastenaire, and R Tixier, "Applications of statistical methods in microanalysis" in *Microanalysis and Scanning Electron Microscopy: Proceedings of the Summer School at St-Martin-d'Heres*, eds. F Maurice, L Meny, and R Tixier, Les Editions de Physique, Orsay, France, 1978.

[8] F Kalfoun, D Ionov, and C Merlet, *Earth Planet Sci Lett* 199 (2002) 49–65.

[9] ES Pearson and HO Hartley, *Biometrika Tables for Statisticians*, vol. 2, Cambridge University Press, London, 1972.

MT